PROTEINS: Structure, Function, and Genetics 37:293–302 (1999)

The Function of Conserved Amino Acid Residues Adjacent to the Effector Domain in Elongation Factor G

J. Daniel Sharer,[1] Homa Koosha,[1] W. Bret Church,[2] and Paul E. March[1]*
[1]*School of Microbiology and Immunology, University of New South Wales, Sydney, Australia*
[2]*Garvan Institute of Medical Research, St. Vincent's Hospital, University of New South Wales, Sydney, Australia*

ABSTRACT **Bacterial elongation factor G (EF-G) physically associates with translocation-competent ribosomes and facilitates transition to the subsequent codon through the coordinate binding and hydrolysis of GTP. In order to investigate the amino acid positions necessary for EF-G functions, a series of mutations were constructed in the EF-G structural gene (*fusA*) of *Escherichia coli*, specifically at positions flanking the effector domain. A mutated allele was isolated in which the wild-type sequence from codons 29 to 47 ("EFG2947") was replaced with a sequence encoding 28 amino acids from ribosomal protein S7. This mutated gene was unable to complement a *fusA^{ts}* strain when supplied in trans at the nonpermissive temperature. In vitro biochemical analysis demonstrated that nucleotide crosslinking was unaffected in EFG2947, while ribosome binding appeared to be completely abolished. A series of point mutations created within this region, encoding L30A, Y32A, H37A, and K38A were shown to give rise to fully functional proteins, suggesting that side chains of these individual residues are not essential for EF-G function. A sixth mutant, E41A, was found to inefficiently rescue growth in a *fusA^{ts}* background, and was also unable to bind ribosomes normally in vitro. In contrast E41Q could restore growth at the nonpermissive temperature. These results can be explained within the context of a three-dimensional model for the effector region of EF-G. This model indicates that the effector domain contains a negative potential field that may be important for ribosome binding. Proteins 1999;37:293–302.** © 1999 Wiley-Liss, Inc.

Key words: *fusA*; *E. coli*; mutagenesis; electrostatic potential; surface charge; homology modeling; ribosomes; translation

INTRODUCTION

Translocation of the ribosome on an mRNA transcript, a fundamental and highly conserved process in protein synthesis, is catalyzed by elongation factor G (EF-G, translocase; EF-2 in archaea and eukaryotes). A member of the GTPase superfamily (1), EF-G binds both GDP and GTP, and possesses an intrinsic ability to hydrolyze the γ phosphate of GTP. EF-G(GTP), conventionally termed the active state, specifically recognizes and binds 70S ribosomes containing a peptidyl-tRNA in the A site.[2,3] Many details concerning this process remain to be established. For example the exact roles of EF-G binding to 70S ribosomes and GTP-hydrolysis are still controversial.[4,5]

EF-G, like all GTPases, contains three highly conserved sequence motifs (G1, G3, and G4) which together form the nucleotide binding/hydrolysis pocket.[6] In addition, there is a fourth motif (G2) between G1 and G3 with a sequence that is specific to elongation factors.[1] This region is commonly referred to as the effector domain, based on the analogous region of p21ras,[7] which is required for interaction with effector molecules.[7,8] Bacterial EF-Gs share a high degree of sequence similarity in the positions separating G1 and G2, with considerably less conservation evident between G2 and G3. In contrast, the Tu elongation factors (EF-Tu) are characterized by the opposite pattern of conserved sequences, that is, positions between G1 and G2 are noticeably less similar than G2/G3-spanning sequences. EF-Tu binds the ribosome at virtually the same site as EF-G,[9,10] but at a temporally distinct stage of translation. Therefore, these sequence patterns may be significant in terms of conferring functional specificity.

Based in part on these sequence comparisons, a series of chimeric proteins have previously been constructed between EF-G and LepA,[11] an *Escherichia coli* GTPase of unknown function which contains an elongation factor-like G2 domain.[12,13] Analysis of these chimeras has suggested that positions between G1 and G2 are important for normal EF-G function.[11] This is similar to the eukaryotic protein Krev, which possesses an effector domain sequence identical to that of p21ras, yet can revert the morphological phenotype of ras-transformed cells when overexpressed.[14] This activity has been shown to absolutely require two small clusters of Krev-specific amino acids which flank the G2 domain, [15] demonstrating that residues proximal to the effector region, but outside its defined boundaries, can be highly important for protein function.

In order to examine the functional significance of certain effector-domain flanking amino acid residues of *E. coli* EF-G we have performed site-specific mutagenesis on selected positions within this region. These mutations were initially analyzed for the ability to functionally replace the wild-type protein; interesting mutations were

Grant sponsor: Australian Research Council; Grant number: A09600894.
*Correspondence to: Paul E. March, School of Microbiology and Immunology, University of New South Wales, Sydney, Australia 2052. E-mail: P.March@UNSW.Edu.Au
Received 22 January 1999; Accepted 18 May 1999

further characterized with respect to GTP crosslinking and ribosome binding relative to the normal protein. Our results indicate that the positions located between the defined boundaries of G1 and G2 in EF-G are required for ribosome binding.

MATERIALS AND METHODS

Materials

ATP, GTP, and GTP(γ)S were purchased from Sigma Chemicals. 8-N_3[α-^{32}P]GTP was supplied by ICN Biomedicals. Glutaraldehyde activated silicate beads were obtained from Boehringer Mannheim. Enzymes were supplied by Boehringer, GIBCO BRL, and New England Biolabs. Western blot detection was performed utilizing the ECL system from Amersham. Protein determinations were performed using BioRad reagents. Purified 70S ribosomes were generously provided by Robert Traut (Department of Medical Biochemistry, University of California-Davis).

Bacterial Strains and Plasmids

Standard procedures were used for cell growth and medium preparation; all media, either liquid or solid agar, was supplemented with 50 μg/ml ampicillin (LA_{50}). Strain SB221 (*lpp hsdR* Δ*trpE5 leuB6 recA1/F′ lacI^q lac$^+$*)[12] was utilized for its high competency following $CaCl_2$ treatment. PEM100,[16] which was utilized for all complementation analysis, is a derivative of JM83[16] containing the temperature sensitive *fusA100* allele.[16] Plasmid pUC4G[16] is a pUC19[17] derivative containing the *fusA* structural gene from pLL145.[18]

PCR Mutagenesis

All mutations were constructed in pUC4G. Sequential PCR mutagenesis was carried out essentially as described[19] utilizing Vent DNA Polymerase (New England Biolabs). See Figure 1 for the sequences of primers used in this work, along with a schematic depicting the region of *fusA* containing sites targeted for mutagenesis. Sequential PCR required two separate initial reactions, one utilizing primers [1] and [B], the other using primers [2] and [A] (as shown in Fig. 1). The amplified, overlapping products of the two initial reactions were gel purified and combined in a second reaction, along with primers [1] and [2], producing the final full length product. The 5′ region of *fusA* containing all positions targeted for mutagenesis is flanked by *Nco*I restriction sites on either side; these are the only NcoI sites on the entire plasmid. Following completion of the sequential PCR mutagenesis procedure the full-length product was digested with *Nco*I. The resulting 347-bp DNA fragment was gel purified and ligated into pUC4G, which had been cut with the same enzyme and gel purified away from the smaller fragment. The ligation reaction mixture was used to transform competent SB221 cells and selection was performed on LA_{50} plates. Plasmid DNA was isolated from selected transformants and screened via restriction analysis for correct orientation of the insert. Final constructs were sequenced (utilizing a DuPont Genesis 2000 automated sequencing system, and an ABI Model 373A automated sequencing system) in order to verify the presence of the desired mutation, and to ensure the absence of any polymerase-derived alterations. The mutated derivatives of pUC4G were tested for the ability to functionally replace EF-G by transformation into competent PEM100 and incubation at the permissive (30°C) and nonpermissive (42°C) temperatures on LA_{50} plates.

Preparation of Whole Cell and Ribosome-Free Lysates

Individual noncomplementing mutated pUC4G plasmids were transformed into PEM100 cells and grown overnight on solid LA_{50} agar at 30°C. Single colonies were removed from the plates after approximately 18 h and used to inoculate 2 ml LA_{50} liquid cultures, which were grown for 12 h at the same temperature. Half of these cultures were used to inoculate 50 ml liquid LA_{50} cultures (preequilibrated to 30°C) which were then grown to a turbidity corresponding to approximately 35 Klett units. At this point the cultures were induced with isopropyl-β-D-thiogalactoside (IPTG) at a final concentration of 2 mM. After a 30-min induction half the volume of each culture was rapidly shifted to 42°C by transferring the cells to separate flasks prewarmed to the desired temperature. Following shift the cells were incubated for an additional 3 to 4 h, then harvested by low speed centrifugation. Preparation of cell lysates was carried out entirely at 0°C. Cell pellets designated to be prepared as whole cell lysates were resuspended in buffer #1 (20 mM HEPES pH 7.5, 1 mM EDTA, 100 mM NaCl, 10 mM $MgCl_2$, 0.1 mM PMSF), incubated at 0°C for 30 min with 50 μg lysozyme, and lysed via sonication. Unlysed cells and debris were removed by centrifugation for 4 min at 16,000 X g. Total protein concentration of the supernatant was determined and aliquots were frozen at −0°C. Cell pellets to be prepared as ribosome-free lysates were resuspended in buffer #2 (50 mM Tris, pH 7.5, 100 mM KCl, 10 mM $MgCl_2$, 50 mM NH_4Cl, 0.1 mM PMSF), lysed via sonication, and subjected to ultracentrifugation at 100,000 X g for 4 h to remove ribosomal proteins. Each lysate was analyzed via sodium dodecyl sulfate-polyacrylamide gel electrophoresis (SDS-PAGE) to verify removal of ribosomal proteins prior to further use.

GTP Crosslinking

Detection of nucleotide binding using the photoactivatable GTP analog 8-N_3[α-^{32}P]GTP has been described previously.[11,20] Briefly, whole cell lysates containing either wild-type or mutant EF-Gs were mixed with 0.5 μCi 8-N_3[α-^{32}P]GTP and 1 mM ATP in buffer #1 at 0°C for 10 min (12 μl total volume). In addition, control tubes contained 1 mM GTPγS. The total protein amounts of each lysate used in the assay were as follows: pUC19(30°C and 42°C): 5 μg; pUC4G(30°C): 0.5 μg; pUC4G(42°C): 0.3 μg; EFG2947(30°C): 0.66 μg; EFG2947(42°C): 5 μg. Mixtures were then UV irradiated at a pathlength of 2 cm for 5 min and immediately heated to 95°C for 3 min in 5X SDS loading buffer. Samples were then subjected to SDS-PAGE, stained with Coomassie brilliant blue,

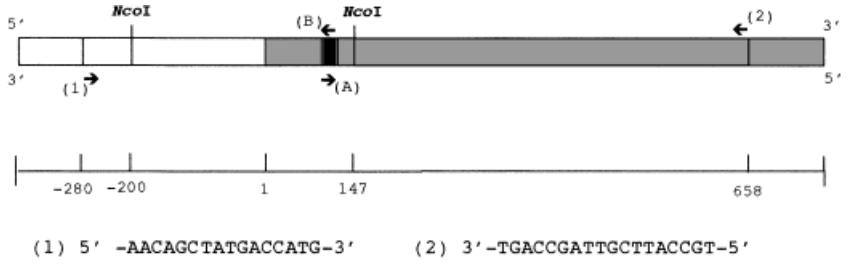

(3) **L30A** (91–93)
3A) 5′-CCGAACGTATTGCGTTCTACACCGGT-3′
3B) 3′-GATGGCTTGCATAACGCAAGATGTGG-5′

(4) **Y32A** (97–99)
4A) 5′-CTGTTCGCCACCGGTGTAAACCAT-3′
4B) 3′-CTTGCATAAGACAAGCGGTGGCCA-5′

(5) **H37A** (112–114)
5A) 5′-GTAAACGCTAAAATCGGTGAAG-3′
5B) 3′-GGCCACATTTGCGATTTTAGCC-5′

(6) **K38A** (115–117)
6A) 5′-AACCATGCAATCGGTGAAGTTCAT-3′
6B) 3′-TGGCCACATTTGGTACGTTAGCCA-5′

(7) **E41A** (124–126)
7A) 5′-CCATAAAATCGGTGCAGTTCATGACGGC-3′
7B) 3′-GGTATTTTAGCCACGTCAAGTACTGCCG-5′

(8) **E41Q** (124–126)
8A) 5′-CCATAAAATCGGTCAAGTTCATGACGGC-3′
8B) 3′-GGTATTTTAGCCAGTTCAAGTACTGCCG-5′

Fig. 1. PCR mutagenesis: the region of *fusA* on pUC4G targeted for amplification, along with associated primer sequences. Diagram indicates the 5′ end of *fusA* on pUC4G, along with flanking PCR primers [1] and [2], and the internal primers [3] through [8] containing the nucleotide changes required for the indicated residue changes (underlined) as described in Materials and Methods. The shaded region initiating at base position #1 indicates the *fusA* translated region. The solid black box indicates the boundaries of the mutations described in this report. The range of numbers in parentheses after each mutant position (for example, 91–93 after L30A) indicates the nucleotide position of the codon which was altered. Primers (A) and (B) show the annealing positions and orientations generally representative of all such primers used in this work and do not indicate the position of any specific primer. For reference, the scale below the upper box indicates nucleotide positions numbered from the A (position 1) of the initiation codon.

destained with 10% acetic acid, and photographed. The dried gel was subsequently exposed to Kodak X-AR5 film for 18.5 h to visualize EF-G bands covalently bound to the radioactive GTP analog.

Ribosome Binding Assay

Determination of ribosome association with both wild-type and mutant EF-Gs was performed as described.[21] Briefly, 5 mg of Boehringer silicate beads were incubated with 150 µg purified 70S ribosomes and mixed gently at room temperature for 3 h (50 µl final volume). Control beads were processed in the absence of added ribosomes in order to assess relative amounts of nonspecific binding. Unreacted sites were then blocked with 150 mM Tris for 1 h at room temperature, followed by an additional incubation with 50-mM NH_4Cl for 20 min. After extensive washing with buffer #2 the ribosome-bead complexes were incubated with appropriate amounts of ribosome-free lysates containing either wild-type or mutant EF-G, along with 0.3 mM GMP-PNP in buffer #2 (final volume: 150 µl) for 30 min at 4°C. A total of 0.3 µg of each EF-G was present in each binding reaction. The beads were then washed extensively with buffer #2 and heated at 95°C for 3 min in 5X SDS-PAGE loading buffer. Samples of the supernatants were subjected to SDS-PAGE, blotted to nitrocellulose, and visualized using (anti)EF-G serum with the Amersham ECL detection kit.[21]

Three-Dimensional Modeling

The remarkable structural similarity of EF-Tu(GTP) and EF-G(GDP) was used to build a homology model of the p-loop region (residue numbers 39–62).[22] A homology model of the p-loop region was built from EF-Tu.GTP coordinates based on an overall sequence alignment. Homology modeling was performed on a Silicon Graphics using the visualization software InsightII (version 95) from Biosym/MSI Inc. Homology[23] was used for model generation and evaluation. Discover[24] was used for energy minimization. All minimizations, utilized CVFF forcefield. Coordinates were obtained from Czworkowski et al.[25] and the Brookhaven Protein Data Bank.[26] The structural model of the mutated proteins E41A and E41Q were obtained by replacing the E41 in the model of nonmutated *E. coli* EF-G with either Alanine or Glutamine. To construct a model for EFG2947 the side chains of residue numbers 29–47 were replaced with corresponding residues found in EFG2947. The calculation of electrostatic potential was carried out using the Finite Difference Poisson-Boltzmann method.[27] The charges of ionized groups were assigned to −1 for side chains of D and E, +1 for K, and R; and 0.5 for H. The assignment of

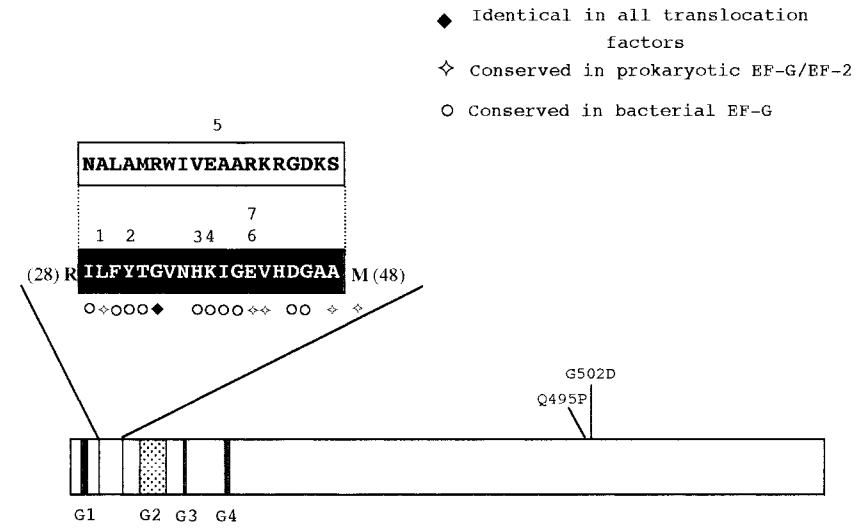

Mutations:	Complementation (PEM100):
1. L30A	+
2. Y32A	+
3. H37A	+
4. K38A	+
5. EFG2947	–
6. E41A	–/+
7. E41Q	+

Fig. 2. Results of PCR mutagenesis. Schematic showing the relative positions of the effector domain-flanking sites changed in this study. Mutations 1 through 7 are listed below and their positions relative to the effector domain are shown above. The wild-type sequence of codons 28 to 48 is shown in white lettering while the substituted sequence found in EFG2947 is given in black lettering, above. The amino acid conservation within this region is indicated, along with conserved motifs (G1, G2, G3, and G4) and the positions of the C-terminal ribosome binding mutants described in the text. Results of complementation analysis in PEM100 are also shown ("+" indicating normal growth at 42°C relative to wild-type pUC4G, "–" no growth, "–/+" very poor growth).

atomic radii was set using the default parameters. The ionic strength was 145 mM, and the dielecteric constants for the protein interior and surrounding solvent were 2 and 80, respectively. The interior and exterior of the protein were defined by the solvent-accessible surface area. A solvent radius of 1.4 Å was used. Each molecule was centered in a grid defined of the dimensions of 65 Å × 47 Å × 53 Å.

RESULTS

Site-specific PCR Mutagenesis of Effector Domain-Flanking Residues in EF-G

As mentioned previously, the region of interest in this study was defined by earlier work with EF-G/LepA chimeras, which implicated the ca. 28 amino acid residues located between G1 and G2 as being essential for EF-G function.[11] Analysis of sequence alignments between *E. coli* EF-G, other bacterial EF-Gs, archael EF-2s, and translocation factors in eukaryotic organisms led to identification of amino acid residues within this region which were either 100% identical in all cases, conserved (allowing for conservative replacements) within bacterial and archael elongation factors, or conserved within bacterial species only. Criteria for selection of positions to mutate took into account both the extent of evolutionary conservation and the chemical nature of amino acid side chains. The primary goal was to replace amino acids containing large or bulky side chains with alanine residues. Ultimately, the following five positions were selected: L30, Y32, H37, K38, and E41. Sequential PCR (Figs. 1 and 2) was employed to introduce the necessary changes in the *fusA* coding sequence; this technique proved to be advantageous in terms of being both fast and effective. However, during the course of this work, an unexpected primer hybridization event occurred which resulted in amplification of a chimeric sequence. This sequence encodes a mutated EF-G containing a complete substitution of codons 29 to 47. The EF-G sequence was replaced by a sequence

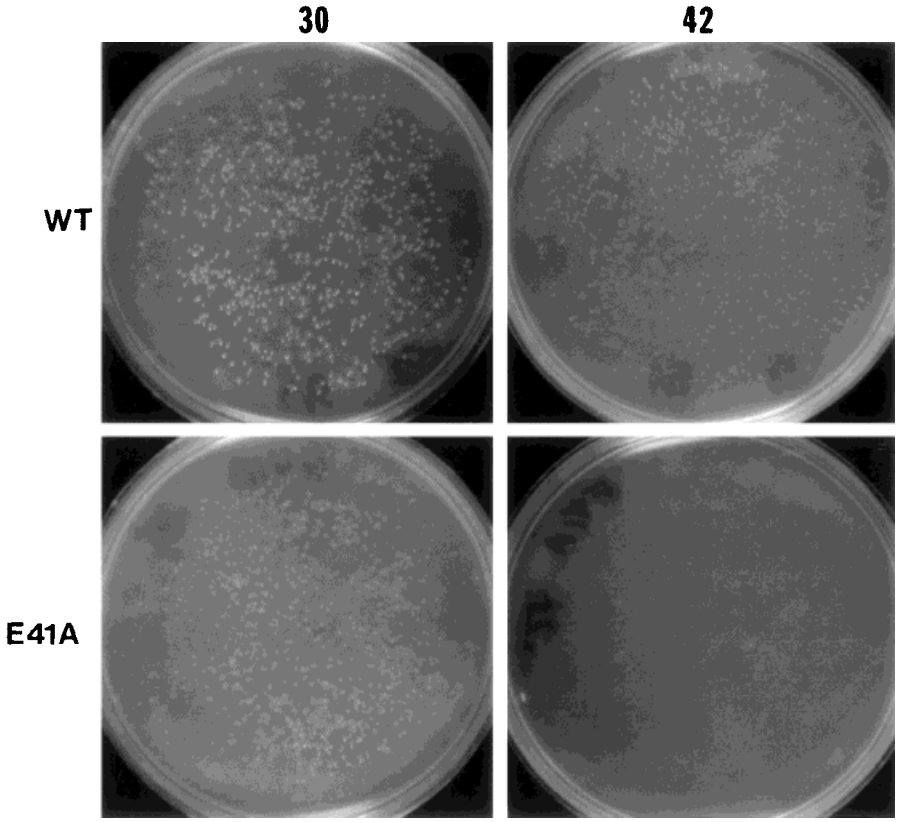

Fig. 3. Growth properties of PEM100 cells harboring vectors that express E41A and wild-type EF-G. Competent PEM100 cells were transformed with approximately 5 ng of either pUC4G (top row) or E41A (bottom row) then grown on LA_{50} plates at 30°C and 42°C (as indicated at the top of the figure) for 17 h.

derived from the region encompassing codons 97 to 116 from the gene upstream of EF-G (encoding ribosomal protein S7). The resulting hybrid protein was referred to as EFG2947 (Fig. 2) and it was employed to examine the affect of wholesale substitution of this region. In no other case was this result repeated, and in all instances the entire amplified region was sequenced to verify the fidelity of the DNA polymerase utilized in this work (no errors attributable to polymerase misincorporation were identified in over 3×10^3 bases amplified and sequenced).

Complementation Analysis of Mutated EF-G Genes

Strain PEM100 contains the *fusA100* allele, which encodes a temperature sensitive version of EF-G. Wild-type EF-G, when supplied in trans from pUC4G, can functionally replace the defective protein at the nonpermissive temperature (42°C). It should be noted that this growth rate is slightly slower than that of normal cells containing the chromosomal fusA allele, due to the extremely high copy number of pUC4G (at 42°C the ColE1 origin of this plasmid produces $>$ 200 copies per cell[17]). As an initial screen for functionally compromised proteins each mutated allele (in pUC4G) was tested for the ability to complement PEM100 at the nonpermissive temperature. As summarized in Figure 2, L30A, Y32A, H37A, and K38A all promoted cell growth at 42°C which was indistinguishable from wild-type pUC4G controls. EFG2947, however, was completely unable to rescue growth at the nonpermissive temperature. E41A-transformed cells formed microcolonies on LA50 plates incubated at 42°C for 17 h (Fig. 3), and growth was also initially somewhat slower at 30°C than that of cells containing pUC4G (data not shown), though this difference was nearly undetectable after 17 h (Fig. 3). In order to examine the function of residue 41 more carefully the mutation E41Q was constructed and observed to be only slightly deficient in growth compared to the nonmutant control. The alteration of a glutamic acid residue to an alanine changes the size and charge of the side chain, whereas a change to glutamine only alters charge.

UV Crosslinking of EF-G Proteins to 8-N_3[α-^{32}P]GTP

A plausible explanation for the nonfunctional phenotype of EFG2947, and the slowly complementing phenotype of E41A, was that these mutations had grossly disrupted the overall structure of the nucleotide-binding domain, resulting in total or partial loss of function. This consideration seemed much more likely, of course, for EFG2947, in which multiple residue changes were made, as opposed to E41A, which contains only a single amino acid replacement. In order to address this possibility the ability of EFG2947 to bind a radioactive, photoactivatable analog of GTP (8-N_3[α-^{32}P]GTP) was assessed and compared to the wild-type protein. As shown in Figure 4 panel A, whole cell lysates containing the EFG2947 version of pUC4G, induced with 2 mM IPTG and either retained at 30°C or shifted to 42°C for

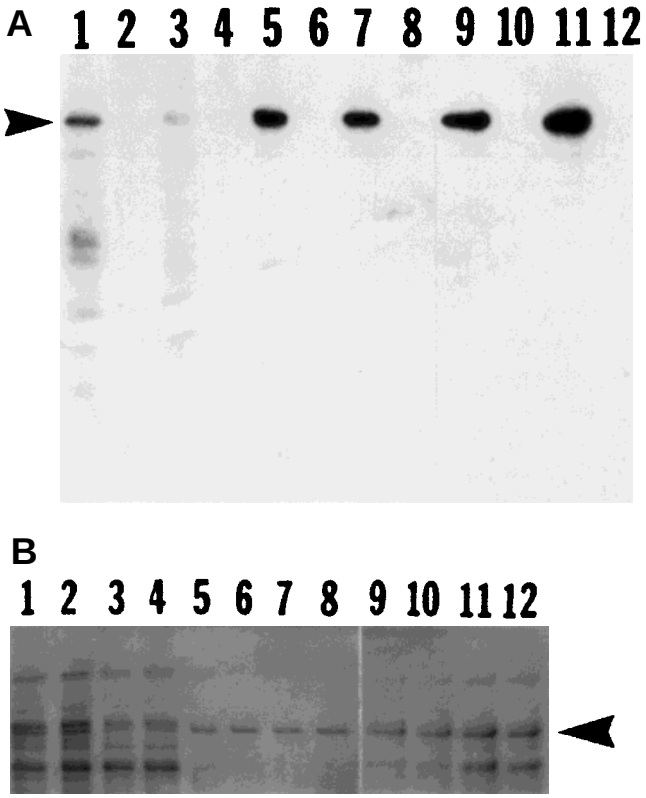

Fig. 4. Nucleotide crosslinking to EF-G in cell lysates. **A:** PEM100 induced with IPTG was incubated at 30°C (lanes 1, 2, 5, 6, 9, and 10) or shifted to 42°C for 3 h (lanes 3, 4, 7, 8, 11, and 12). Following growth, whole cell lysates were prepared and incubated with 8-N_3[α-^{32}P]GTP in the presence (lanes 2, 4, 6, 8, 10, and 12) or absence (lanes 1, 3, 5, 7, 9, and 11) of GTPγS, UV irradiated, and separated on SDS-PAGE as described under Materials and Methods. The resulting autoradiogram shown in panel A contains lysates with the following plasmid types: lanes 1–4, pUC19; lanes 5–8, pUC4G; lanes 9–12, EFG2947. The position of EF-G is indicated by the arrowhead. **B:** Photograph of the Coomassie blue stained SDS-polyacrylamide gel used to obtain the the autoradiogram shown in panel A. Contents of each lane are as described in panel A. The arrowhead indicates the position of EF-G on the gel.

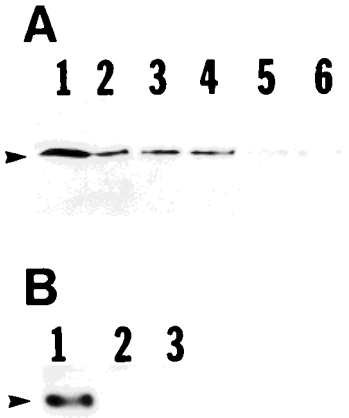

Fig. 5. EF-G:70S ribosome binding assay. PEM100 cells containing either pUC19, pUC4G, pUCE41A, or pUCEFG2947 were induced with IPTG, shifted to 42°C for 4 h, processed as ribosome-free lysates, and tested for ribosome binding as described under Materials and Mehtods. The position of EF-G is indicated by the arrowhead. **A:** immunoblot containing lysates incubated with ribosome beads (lanes 1, 3, and 5) or control beads (lanes 2, 4, and 6). Lanes 1 and 2: pUC4G lysate. Lanes 3 and 4: E41A lysate. Lanes 5 and 6: EFG2947 lysate. **B:** immunoblot containing approximately 5 ng pure EF-G (lane 1) and a PEM100 lysate (shifted to 42°C as previously described) containing pUC19 incubated with ribosome beads (lane 2) or with control beads (lane 3).

3 h, could clearly be crosslinked to the GTP analog (lanes 9 and 11). This interaction was effectively competed by the addition of nonhydrolyzable GTPγ S, as shown in lanes 10 and 12. The assay results for the wild-type protein appeared indistinguishable when it was expressed in pUC4G under the same conditions (Fig. 4A lanes 5–8). In order to discriminate between the radioactive signal arising from endogenous EF-G and that expressed from the plasmid, these experiments were performed in the *fusA100* strain PEM100. Using this *fusA*^{ts} strain it was shown previously that within 3 h after shifting to 42°C the cellular content of endogenous EF-G had been reduced to undetectable levels.[16] In Figure 4 the signal arising in the crosslinking assay from chromosomally derived EF-G is shown in lanes 1 and 3 for cells cultured at 30° and 42°C (for 3 h) respectively. The amount of lysate employed in these particular reactions (lanes 1–4) was about tenfold higher than the amount employed in all other assays except those shown in lanes 11 and 12. A comparison of lysates prepared from cells grown at 42°C (lanes 3, 4, 7, 8, 11, and 12) indicates that nearly all of the radioactivity incorporated into EF-G protein at 42°C was present in plasmid-derived protein. E41A was not assayed for nucleotide binding because the mutation occurs within the region already altered much more drastically in EFG2947. These results suggest that the EF-G nucleotide binding site was not adversely affected by the EFG2947 mutation.

Ribosome Binding of E41A and EFG2947 Is Deficient

The relative affinities of both wild-type and mutated EF-Gs for 70S ribosomes were evaluated utilizing a novel technique described previously.[21] Other methods have been based on the ability of fusidic acid to cause EF-G to become irreversibly bound to the ribosome,[28,29] however, assays of this type cannot distinguish between defects in the fusidic acid binding site on EF-G versus actual deficiencies in ribosome binding. The method employed here detects EF-G:ribosome interaction directly through covalent binding of purified 70S ribosomes on silicate beads, incubating these beads with an appropriate ribosome-free EF-G lysate (in the presence of the nonhydrolyzable GTP analog GMP-PNP), washing extensively, and visualizing bound EF-G via immunoblotting. Control reactions were performed utilizing beads that had not been previously incubated with ribosomes, in order to account for nonspecific binding of EF-G. The amount of each EF-G protein present in the assay was equalized based on comparison of

Coomassie blue stained protein bands on SDS-polyacrylamide gels (data not shown). The results of these experiments are shown in Figure 5. Wild-type EF-G clearly associated with the beads in a ribosome-specific manner (part A; compare lanes 1 and 2), while both E41A (lanes 3 and 4) and EFG2947 (lanes 5 and 6) did not. Endogenous EF-G from the *fusA100* allele was not a factor in these assays, as shown in part B, due to the instability of this protein at 42°C (see above).

Nonspecific binding appeared to be similar in both wild-type EF-G and E41A, while EFG2947 had a much lower affinity for untreated beads (Fig. 5, lanes 2, 4, and 6). This was consistent with the observation that EFG2947 eluted from an ion exchange matrix under different ionic conditions than either the normal protein or the other mutants (data not shown). The 29–47 substitution probably results in a change in the overall charge of the protein, as well as altering the surface characteristics at this particular region. These observations were consistent with conclusions drawn from three-dimensional modeling as described in the following section.

Three-Dimensional Model for the P-Loop Region

Relating the function of residue 41 to the three dimensional structure of EF-G was not possible because this region of the crystal structure has not been resolved.[25,30] A model is proposed here (Fig. 6) using available coordinates from highly related structures (see Methods section). To model structural alterations in the region of the introduced mutations computer modeling was employed to compare E41A, E41Q, and EFG2947 to the unmutated protein. The electrostatic potentials of EF-G(GDP), E41A, E41Q, and EFG2947 were calculated using the structural models. The analyses indicate that the changes in mutated proteins do not affect the structure, however the accessible surface area and electrostatic potential are affected (Fig. 7). The E41A mutation decreases surface accessible area resulting in distortion of hydrogen bonding character of the putative ribosome binding region. In the case of EFG2947, the changes were significant at residue numbers 35, 44, and 46.

Figure 7 shows the electrostatic potential surface of each model. The potential field of the putative ribosome-binding region was different in all four cases. There is a well-defined negative potential field in the unmutated protein that extends out into the solvent (shown in Fig. 7A). This large negative potential field is no longer seen in E41A and EFG2947 (Fig. 7 B and D). In EFG2947 the region adjacent to position 41 now appears as a positive field. The negative field seen in the wild-type protein may be important for binding to the ribosome, and thus the substitutions found in EFG2947, and E41A would be expected to ablate the interaction between EF-G and the ribosome. The substitution of E41Q did not dramatically affect the electrostatic potential field and therefore, ribosome binding would not be expected to be affected.

DISCUSSION

In this report, EF-G effector domain-flanking amino acid residues required for functional ribosome interaction were investigated. A mutated EF-G protein characterized by complete substitution of residues 29 to 47, EFG2947, was unable to complement the *fusA*^{ts} strain PEM100 at 42°C and was apparently entirely unable to bind 70S ribosomes in vitro. A second mutated protein containing a single E to A substitution at position 41 (E41A) was unable to efficiently rescue growth in PEM100 at 42°C. The protein was also clearly deficient in ribosome binding in vitro. These observations were apparently not attributable to wholesale structural disruption of the nucleotide-binding domain since 8-N_3[α-^{32}P]GTP binding was not adversely affected in EFG2947. The caveat to this conclusion is that the cross-linking assay may not be sensitive to smaller scale structural changes.

Homology-based structural modeling was employed to construct a model for this region of *E. coli* EF-G (Figs. 6 and 7). This model suggests that electrostatic interactions are important for modulating ribosome interactions in the area surrounding residue 41. The presence of a negative surface potential correlated directly with functional assays such as ribosome binding (Fig. 5) and the ability to rescue the *ts* growth defect in PEM100 (Figs. 2 and 3).

In recent experiments hydroxyl radical probing has been employed to map the location and orientation of EF-G on ribosomes in the posttranslocational state.[31] There was a clear partitioning of sites on EF-G between 16S and 23S rRNA as shown by the distribution of rRNA targets relative to the various EF-G probing positions. Based on these data, the EF-G binding site was mapped to a space between the two ribosomal subunits. The location and orientation was very similar to that observed for the EF-Tu ternary complex, determined independently by electron microscopy reconstruction methods.[32] The G-domain of EF-G faces the 50S subunit. It was adjacent to rRNA elements including the sarcin loop and elements of stalk. The nearest neighbor of EF-G Domain 2 was the small subunit, near the binding site of protein S4. Domain 4 was positioned very near elements of the decoding center in the A site.[31] The surface of EF-G that interacts with 30S subunit was defined by seven positions that target 16S rRNA including residue number 37, and residue number 65 of effector region.[31] Although the alteration of H37 to alanine had no measurable affect in vivo according to our findings this region is obviously important because alteration of position E41 does affect EF-G function in vivo and in vitro.

Richter Dahlfors and Kurland have described two mutated alleles of *fusA* that produce EF-Gs that are deficient in ribosome interaction according to kinetic analysis.[33] One of these mutated alleles (encoded by *fusA12*) arose from two point mutations; position 66 was changed from A to V, and position 88 was altered from T to A.[34] Analysis of structural data has led to the hypothesis that these changes may interfere with flexibility and function of the effector region.[35] The second allele *fusA20* results in conver-

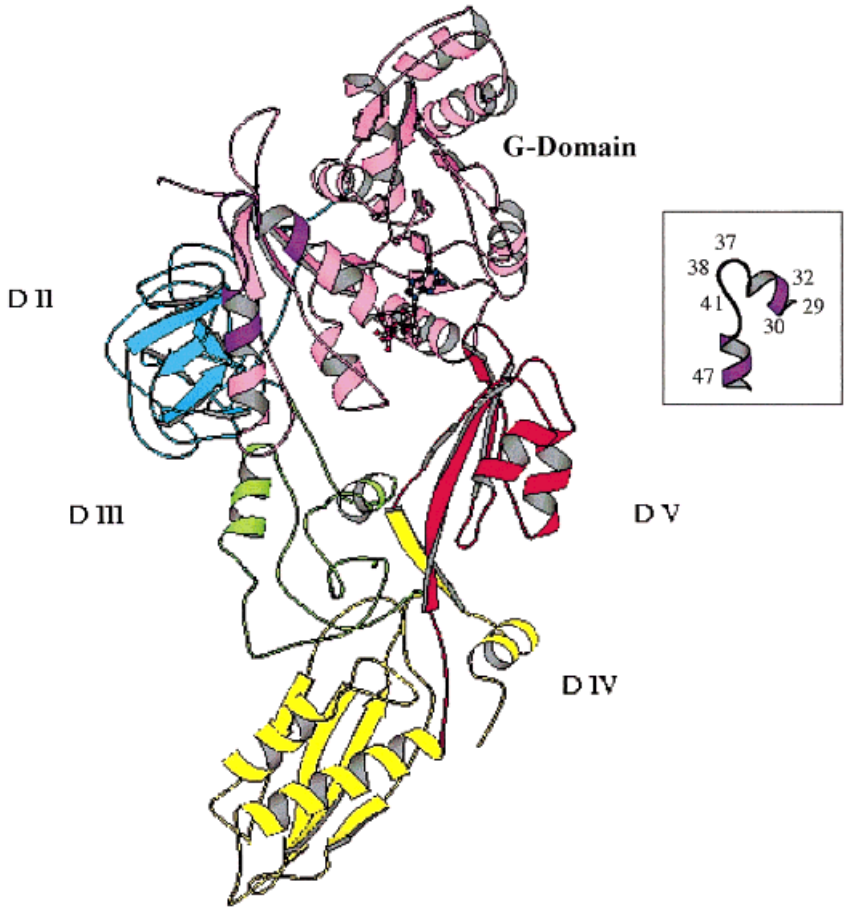

Fig 6. Model for the three dimensional structure EF-G is shown using Molscript.[38] The model contains five domains (G-domain; pink, includes the G′ subdomain), Domain II (D II, blue), Domain III (D III, green), Domain IV (D IV, yellow), and Domain V (D V, red). The model for the effector region of the G-domain is shown in purple. The inset shows the effector region in isolation with residue positions indicated. GDP is shown in ball and stick representation.

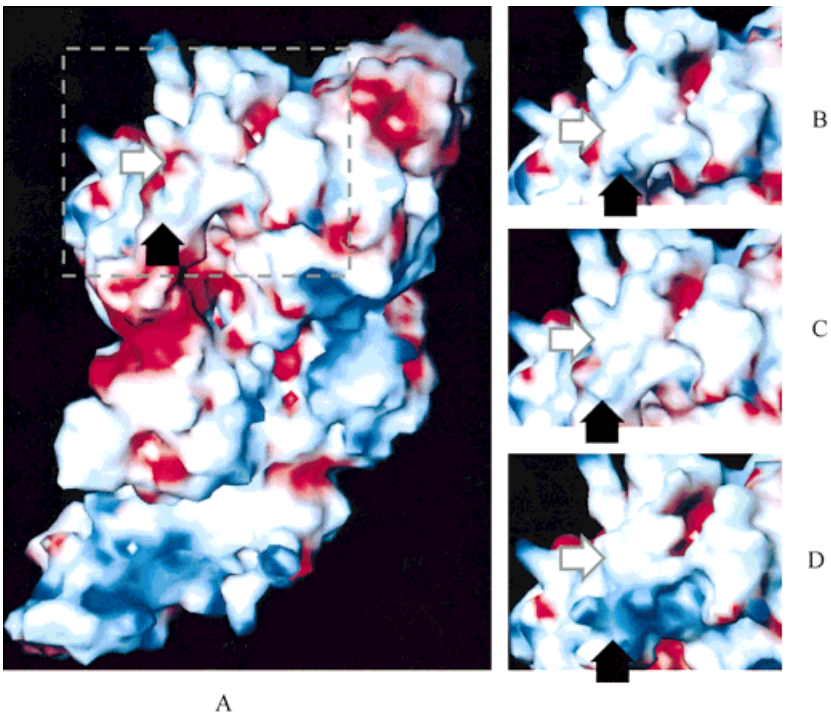

Fig 7. The electrostatic surface potentials of the mutant and wild-type EF-Gs. **A** shows the surface potential of the wild-type protein. The region of the insets shown in B, C, and D is indicated by the dashed lines in A. **B** shows the surface potential of E41A; **C**, E41Q; and **D**, EFG2947. The negative potential is shown in red and the positive potential in blue. The white arrow indicates negative potential near residue 41 that is lost in the mutants. The black arrow indicates a region that becomes strongly positive in E41A and EFG2947.

sion of position 121 from Q to R.[34] In the crystal structure of EF-G this position is located within a cavity bordered by the G domain, along with domains 3 and 5. It has been proposed that this pocket may form part of the binding site for fusidic acid.[36] Q121 is in helix C_G and it directly contacts the residue corresponding to position H17 in *T. thermophilus* EF-G. This interaction may be important for stabilization of the nucleotide binding site.[35] Whether it is necessary for ribosome association directly or indirectly remains to be established, however, it is important to note that Q121 is invariant in EF-G and EF-2 sequences.

The crystal structure of EF-G(GDP)[25,30] reveals that the protein is approximately 110 Å long, consisting of a G domain oriented near the "top" of the molecule, an associated G domain insert just above, and three intriguing domains descending below, terminating at the domain 4 "tail". Residues 29 to 47 in EF-G(GDP) map to a conserved alpha helix and the putative effector loop structure located in the G domain of the protein. Residues 39 to 41 form the beginning of the loop at the end of the helix and are exposed on the surface; residues 42 to 65 are disordered and could not be assigned but are presumably exposed also. Such disorder often reflects structural flexibility, which is characteristic of the analogous regions in both EF-Tu and p21Ras, where extensive conformational change following GTP hydrolysis has been shown to occur.[36,37] Recent pre-steady state kinetic experiments show clearly that GTP hydrolysis occurs before translocation and accelerates translocation more than 50 fold relative to that observed with nonhydrolizable GTP analogs.[5] These new kinetic experiments require a reevaluation of the role of GTP hydrolysis in translocation, suggesting instead that a conformational transition in EF-G itself is in some way coupled to translocation. This conclusion was not supported by the study of Czworkowski and Moore.[4] They concluded that EF-G may undergo little structural reorganization during the translocation step.

The data presented indicates that residues flanking the G2 domain of EF-G are required for proper interaction with 70S ribosomes. These studies highlight the importance of understanding the functional role of the effector region in EF-G.

ACKNOWLEDGMENT

The authors would like to thank Yan Hou for technical assistance.

REFERENCES

1. Bourne HR, Sanders DA, McCormick FM. The GTPase Superfamily: a conserved switch for diverse cell functions. Nature 1990;348: 125–132.
2. Liljas A. In: The ribosome: structure, function, and evolution. Hill WE, Dahlberg A, Garrett RA, Moore PB, Schlesinger D, Warner JR, editors. The ribosome: structure, function, and evolution. Washington, D.C.: American Society for Microbiology; 1990. p. 309–317.
3. Kaziro Y. The role of Guanosine 5'-Triphosphate in polypeptide chain elongation. Biochim Biophys Acta 1978;505:95–127.
4. Czworkowski J, Moore PB. The conformational properties of elongation factor G and the mechanism of translocation. Biochemistry 1997; 36:10327–10334.
5. Rodnina MV, Savelsbergh A, Katunin VI, Wintermeyer W. Hydrolysis of GTP by elongation factor G drives tRNA movement on the ribosome. Nature 1997;385:37–415.
6. Bourne HR, Sanders DA, McCormick FM. The GTPase Superfamily: conserved structure and molecular mechanism. Nature 1991; 349:117–127.
7. Lowy DR, Willumsen BM. Function and regulation of ras. Annu Rev Biochem 1993;62:851–891.
8. Feig L, Schaffhausen B. Signal transduction. The hunt for Ras targets. Nature 1994;370:508–509.
9. Moazed D, Robertson JM, Noller HF. Interaction of elongation factors EF-G and EF-Tu with a conserved loop in 23S RNA. Nature 1988;334:362–364.
10. Weijland A, Harmark K, Cool RH, Anborgh PH, Parmeggiani A. Elongation factor Tu: a molecular switch in protein biosynthesis. Mol Microbiol 1992;6:683–688.
11. Yaskowiak ES, March PE. Small clusters of divergent amino acids surrounding the effector domain mediate the varied phenotypes of EF-G and LepA expression. Mol Microbiol 1995;15:943–953.
12. March PE, Inouye M. Characterization of the lep operon of *E. coli*: identification of the promoter and the gene upstream of the signal peptidase I. J Biol Chem 1985;260:7206–7213.
13. March PE, Inouye M. GTP-binding membrane protein of *Escherichia coli* with sequence homology to initiation factor 2 and elongation factors Tu and G. Proc Natl Acad Sci USA 1985; 82:7500–7504.
14. Kitayama H, Sugimoto Y, Matsuzaki T, Ikawa Y, Noda M. A ras-related gene with transformation suppressor activity. Cell 1989; 56:77–84.
15. Zhang K, Noda M, Vass WC, Papageorge AG, Lowy DR. Identification of small clusters of divergent amino acids that mediate the opposing effects of ras and Krev-1. Science 1990;249:162–165.
16. Hou Y, Lin Y-P, Sharer JD, March PE. *In Vivo* selection of conditional-lethal mutations in the gene encoding elongation factor G of *Escherichia coli*. J Bacteriol 1994;176:123–129.
17. Messing J. A multipurpose cloning system based on the single stranded DNA bacteriophage M13. Recomb DNA Technol Bull 1979;2:43–48.
18. Zengel JM, Archer RH, Lindahl L. The nucleotide sequence of the *Escherichia coli* gene coding for elongation factor G. Nucleic Acids Res 1984;12:2181–2192.
19. Ausubel FM, Brent R, Kingston RE, et al., editors. Current Protocols in Mol. Biol: Vol. I. Section 8.5.7. New York: Wiley Interscience; 1990.
20. Girsovich AS, Bochkareva ES, Kurtskhalia TV, Pozdnyakov VA, Ovchinnikov YA. Binding of GTP to elongation factor G by photoaffinity labeling. Methods Enzymol 1979;60:726–745.
21. Hou Y, Yaskowiak ES, March PE. Carboxyl-terminal amino acid residues essential for elongation factor-G function in protein synthesis. J Bacteriol 1994;176:7038–7044.
22. Nyborg J, Nissen P, Kjeldgaard M, Thirup S, Polekhina G, Clark BF. Structure of the ternary complex of EF-Tu: macromolecular mimicry in translation. Trends Biochem Sci 1996;21:81–82.
23. Homology 95. User guide. San Diego: MSI.
24. Discover 95.0. User guide. San Diego: MSI.
25. Czworkowski J, Wang J, Steitz TA, Moore PB. The crystal structure of elongation factor G complexed with GDP, at 2.7 Å resolution. EMBO J 1994;13:3661–3668.
26. Bernstein FC, Koetzle TF, Williams GJ, et al. The Protein Data Bank. A computer-based archival file for macromolecular structures. Eur J Biochem 1977;80:319–324.
27. Delphi 95.0. User guide, San Diego: MSI.
28. Kaziro Y, Inoue N, Kuriki K, Mizumoto K, Tanaka M, Kawakita M. Purification and properties of factor G. Cold Spring Harbor Symp Quant Biol 1969;34:385–393.
29. Rohrbach MS, Bodley JW. Isolation of physically and enzymically homogeneous Escherichia coli elongation factor G. Methods Enzymol. 1979;60:606–614.
30. Ævarsson A, Brazhnikov E, Garber M, Zheltonosova J, Chirgadze Y, Al-Karadaghi S, Svensson LA, Liljas A. Three dimensional structure of the ribosomal translocase: elongation factor G from Thermus thermophilus. EMBO J 1994;13:3669–3677.

31. Wilson KW, Noller HF. Mapping the position of translational elongation factor EF-G in the ribosome by directed hydroxyl radical probing. Cell 1988;92:131–139.
32. Stark H, Rodnina MV, Rinke AJ, Brimacombe R, Wintermeyer W, van Heel HM. Visualization of elongation factor Tu on the Escherichia coli ribosome. Nature 1997;389:403–406.
33. Richter Dahlfors AA, Kurland CO. Novel mutants of elongation factor G. J Mol Biol 1990;215:549–557.
34. Johanson U, Hughes D. Fusidic acid-resistant mutants define three regions in elongation factor G of Salmonella typhimurium. Gene 1994;143:55–59.
35. Johnson U, Aeversson A, Liljas A, Hughes D. The dynamic structure of EF-G studied by fusidic acid resistance and internal revertants. J Mol Biol 1996;258:420–432.
36. Berchtold H, Reshetnikova L, Reiser COA, Schirmer NK, Sprinzl M, Hilgenfeld R. Crystal structure of active elongation factor Tu reveals major domain rearrangements. Nature 1993;365:126–132.
37. DeVos AM, Tong L, Milburn MV, et al. Three-dimensional structure of an oncogene protein: catalytic domain of human cH-ras p21. Science 1988;239:888–893.
38. Kraulis PJ. MOLSCRIPT: a program to produce both detailed and schematic plots of protein structures. J Appl Crystallogr 1991;24: 946–950